Model predictive controller for a microrobot navigating in a vascular channel by following a trajectory generated with a joystick device

Meziane Larbi [(1)*], El-Hadi Guechi [(2)], Ahmed Miadi[(3)] ,Youcef Zennir[(4)] and Karim Belahret [(5)]
[(1), (2), (4)] Automatic Laboratory of Skikda, August 20th, 1955 University, SKIKDA, Algeria.
[(3)] Mouloud Mammeri University, Faculty of electrical engineering and informatics, Automatic Department, Tizi-Ouzou, Algeria
[(5)] JUNIA campus Chateauroux, PRISME Laboratory EA 4229, France
{l.meziane, guechi.elhadi,y.zennir }@univ-skikda.dz; ahmed.maidi@gmail.com; karim.belharet@junia.com

Abstract: This article proposes a model predictive control (MPC) for trajectory tracking of a microrobot in a 2D fluidic environment. The reference trajectory is generated using a joystick device and it is estimated using a Luenberger observer. Assuming that the position of the microrobot is measured, the objective is to design an observer-based MPC control capable to track the reference trajectory generated by a joystick device. To optimize the MPC control, we have introduced a quadratic criterion where these parameters are determined to have a specific behavior of the closed loop system. Finally, simulation results are presented here to show the efficiency of the proposed approach.

Keywords: Microrobot, Joystick device, Model predictive controller (MPC),reference trajectory

1. INTRODUCTION

Nowadays, targeted therapeutic treatment is a serious challenge that has been the subject of much attention in the medical domain [1].After decades of research, this practice can considerably improve many medical tasks such as drug targeting while limiting their systematic distribution to the entire human body [2].The magnetic microrobots actuated by electromagnetic actuation (EMA) are artificial systems which play an important role in drug delivery, and they are widely used due both to their perception and action capabilities in the vascular environment [3].The increasing need to reduce the side effects of the drug delivery has stimulated great interest in the control of magnetic microrobots in recent years [4].

Overall, the control strategies for a microrobot can be categorized into three classes: open-loop, teleoperation, and closed-loop. Due the lack of information about the state of the microrobot and the disturbance effects, the two first approaches provide poor performance and loss the tracking accuracy[4-6].Hence, many authors propose a solution by tracking trajectories along the reference trajectory. For example, in [5], the authors present a visual-based automatic controller that incorporates the concept of input-to-state stability (ISS) of microrobot in a fluidic environment. In [6-8],a control scheme that rejects input disturbances to obtain a stable 2D linear model has been developed for the microrobot. In [8], [9], PID control and generalized predictive control were applied to ensure the tracking of a predetermined trajectory. Non-linear controls for trajectory tracking are proposed in [10], [11] and seem to have very efficient robustness qualities. In [12], the authors give an overview of magnetic actuation systems and control methods based on magnetic actuation for microrobots. Although all the work on the proposed controls has been proposed, little work has been done on the design of the observation-based controller. In this context, we can mention the works of [8],[4] who proposed a study and a method of control design based on the Kalman observer and extended state observer respectively. The above works have demonstrated the efficiency of the control used to force the microrobot to follow a reference trajectory without taking into consideration the aspect of minimizing the magnetic energy generated by the electromagnetic device.

However, closed-loop control while minimizing the energy and tracking error is necessary in this type of applications. For this purpose, model-based predictive control is recommended due to constraint handling and optimization of the energy and tracking error.

The use of microrobot in complex vascular networks make the trajectory planning procedure difficult[13], [14]. One of the

solutions is to create a joystick interaction with the practitioner. The haptic-control interaction can lead to many applications such as the interaction between humans and robots and teleoperation to control robots in hostile environments [15], [16]. The haptic interfaces have been used in different ways within the concepts of teleoperation and control of robots [17-19]. Therefore, diverse strategies and architectures of control has been developed, such as control force-position scheme and control force-force scheme [20], [17].In this work, the concept of joystick interaction, based on the Novint Falcon joystick, is used to define the navigation path of the microrobot. For this purpose, an observer-based model predictive control (MPC) strategy is developed to force the microrobot to track the defined trajectory in a 2D environment delivered by joystick device.

The main contributions of this paper are the following:

- A model predictive control (MPC) strategy for the microrobot navigating in a blood vessel is proposed,
- A joystick device is used to define the desired 2D trajectory of the microrobot from the user's movements.

This rest of the paper is organized as follows: **Section 2** presents a dynamic model of microrobot in $\mathbf{2}\boldsymbol{D}$environment. In **section 3**, the observer and control (MPC) are developed, and the overall diagram for closed-loop control of microrobotis presented. The simulation results are presented in the **section 4**. This work is concluded in the **section 5**.

2. MODELING

Let us consider the 2-Dimension ($\mathbf{2}\boldsymbol{D}$) motion of a microrobot in a cylindrical blood vessel, where $P = (x, y)$ and $\dot{P} = (v_x, v_y)$ are respectively the position and velocity of the microrobot along the $\vec{\imath}$ and $\vec{k}$ axis. We notice that close to the optimal trajectory P which is the central line of the vessel, the electrostatic $(F_{el})$and vanderWaals microforces (F_{vdw}) are negligible compared to other relevant forces $(F_d,\ W_a)$[7]. A microrobot of mass m placed in a fluidic environment is subjected to the forces shown in the following figure:

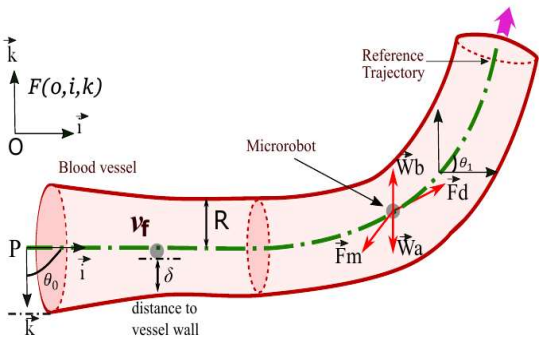

Fig. 1 Forces applied to a magnetic microrobot.

A. Forces

A microrobot navigating in a 2D is subjected to the following forces:

1) **Drag force:** the ferromagnetic microrobot used in this study is spherical of radius r, considering that the fluid has a density equally to that of the microrobot, the buoyancy counteracts the gravitational force W_a. Therefore, both buoyancy and gravitational force can be neglected.

   The drag force defined by the Stokes Law generated by the flowing fluid that opposes the microrobot motion, is simplified as follows [21]:

$$F_d = -6\pi\eta r v_r \quad (1)$$

where $v_r = v - v_f$ represents the relative velocity of the microrobot with respect to the fluid v is the velocity of the microrobot and $v_f$is the velocity of the fluid $(v_f = 0)$.

2) **Apparent weight:** the microrobot is also subject to its apparent weight, which is the contribution of gravity and Archimedes' thrust, it can be expressed as follows:

$$W_a = V(\rho - \rho_f) \quad (2)$$

where V denotes the total volume of the microrobot, ρ its density, $\rho_f$is the density of the fluid and g the oriented vector of the gravity acceleration.

3) **Magnetic force:** a magnetic microrobot that moves with a velocity $\dot{P} = (v_x, v_y)$ in a given magnetic field $\vec{\boldsymbol{B}}$ (see Fig.2) is subjected to a magnetic force that allows it to propel itself along the reference trajectory,

known as the Lorentz force, noted F_m given by (3).

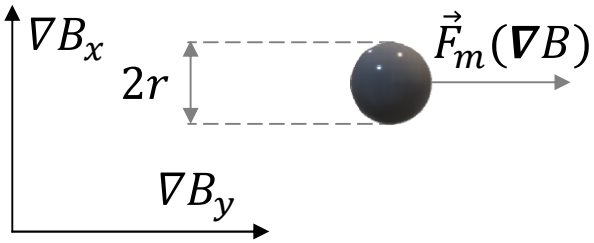

Fig. 2 Microrobot propelled by magnetic force.

$$F_m = V_m(M\nabla)B \quad (3)$$

where V_m is the magnetic volume of the microrobot and M its magnetization.

B. Mathematical model of microrobot

After determining the forces acting on the dynamics of the magnetic microrobot, the dynamic equations of the microrobot can be expressed in different ways and will depend mainly on the used coordinate system. The position vector $P = (x, y)$ will determine the position of the microrobot with respect to the local reference coordinate system $F(O, \vec{\imath}, \vec{k})$. By using the fundamental law of dynamics, we can express all interactions forces, the global linear dynamic model can be reduced to:

$$m\gamma = F_d + F_m \quad (4)$$

where m is mass of the microrobot. Finally, the dynamic model of the considered system, with respect to the frame $F(O, \vec{\imath}, \vec{k})$ is expressed as follows:

$$\begin{cases} m\gamma_x = \gamma_x + \gamma_x \\ m\gamma_y = \gamma_y + \gamma_y \end{cases} \quad (5)$$

Let $\chi = [x \quad v_x]^T$ the state vector denote respectively the microrobot position and velocity along $\vec{\imath}$ axis, and the position and velocity along $\vec{k}$ axis. Using forces expressions (1), (2),(3) and (4), the system (5) can be written as:

$$S_x: \begin{cases} \dot{x} = v_x \\ \dot{v}_x = a_1(v_x - v_{fx}) + b_1 u_x \end{cases} \quad (6)$$

$$S_y: \begin{cases} \dot{y} = v_y \\ \dot{v}_y = a_1(v_y - v_{fy}) + b_2 u_y \end{cases} \quad (7)$$

where $a_1 = a_2 = \frac{6\pi\eta}{m}$ and $b_1 = b_2 = \frac{1}{m}$

The control input $u(t) \in \mathcal{R}^2$ is the force magnetic, by projecting the latter into the reference coordinate system F, so:

$$\begin{cases} u_x = F_{mx} \\ u_y = F_{my} \end{cases} \quad (8)$$

From the dynamic equation (6-7), we obtain the following model in matrix form:

$$S_x: \begin{cases} \dot{X}_x = \begin{pmatrix} 0 & 1 \\ 0 & a_1 \end{pmatrix}\begin{pmatrix} x \\ v_x \end{pmatrix} + \begin{pmatrix} 0 \\ b_1 \end{pmatrix} u_x \\ Y_x = (1 \quad 0) X_x \end{cases} \quad (9)$$

$$S_y: \begin{cases} \dot{X}_y = \begin{pmatrix} 0 & 1 \\ 0 & a_1 \end{pmatrix}\begin{pmatrix} y \\ v_y \end{pmatrix} + \begin{pmatrix} 0 \\ b_1 \end{pmatrix} u_y \\ Y_y = (1 \quad 0) X_y \end{cases} \quad (10)$$

N.B: In the follows, the synthetic control will be developed for the first output $Y_x(t) = x(t)$, because the two subsystems are similar.

In order to be able to use the (MPC) control, we calculate the system response (9) using the transition matrix $e^{A_x t}$. The solution response $X_x(t)$ is given as follows:

$$X_x(t) = e^{A_x t} X_x(0) + \int_0^t e^{A_x (t-\tau)} B_x u_x d\tau \quad (11)$$

where:

$$A_x = \begin{pmatrix} 0 & 1 \\ 0 & a_1 \end{pmatrix}, B_x = \begin{pmatrix} 0 \\ b_1 \end{pmatrix}, C_x = (1 \quad 0)$$

C. Joystick device for reference positions generation

The Falcon developed by Novint is a three-dimensional force feedback controller already exploited in several scientific applications [15]. This system is equipped with three sensors, one on each axis, which measures the precise position along each axis of the handle held by the operator. In this work, the haptic interface was developed under the LabVIEW software using Haptic Library (Fig.4-(a)). The Haptic interfaces using the Novint Falcon 3D joystick have been used in different ways within the concepts of teleoperation and control of robots [23].Therefore, diverse strategies and architectures of control has been developed (see more details [16]):

In this application we considered the position-position architecture. The interface is composed of two parts, firstly, the acquisition part which recovers the measurement signals from the **X**, **Y** and **Z** sensors and which allows us to know the position of the tip in the

space of the scan as well as to deduce the topography. We can see below the schematic diagram of the system, the three outputs corresponding to the displacement of the piezoelectric **X**, **Y** and **Z** measured by the sensors are circled in red, obtained from the National Instruments acquisition library. Secondly, in order to activate the **X** and **Y** piezo movement controls, we have chosen to use the buttons on the Falcon handle. The central button was thus programmed under LabVIEW to drive the **X** and **Y**piezo simultaneously, the two side buttons drive only the **X** piezo and the last button drives the **Y** piezo.

Knowing the environment, the microrobot will be able to move in real time using the positions (X_{ref},Y_{ref}) given by the operator.

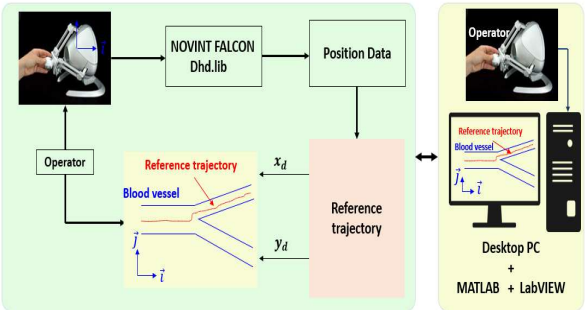

Fig. 3 Basic elements of the Novint Falcon joystick device and their interaction.

The system(6-7) is locally controllable along the reference trajectory (X_{ref}, Y_{ref}),a (MPC) control is used. Summarizes the automatic control algorithm of the microrobot navigating in the human inner ear where the desired reference trajectory is generated by joystick device. The microrobot position can be detected through image processing algorithm. Based on the real-time position feedback, the input current apply to each of the six electromagnetic coils is generated based on the proposed robust control algorithm in order to generate the corresponding magnetic force, this latter, to allow the microrobot to tracking towards the target position with commanded velocity.

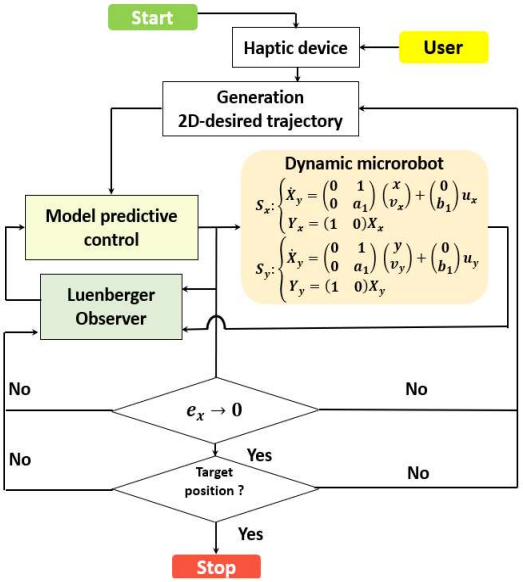

Fig. 4 The overall diagram for closed-loop control of microrobot

3. Observer Based Controller

In our application, the position $P = (x, y)$ of the microrobot can be measured with the aid of a vision system. In this section, an observer-based model predictive control for controlling the state of the system (9) is developed. The first step of this method is to obtain the model predictive (13) using the responses of the microrobot given in (11). Then, a (MPC) linear controller is designed to deal with the tracking problem. Finally, the controller gains are identified based on the behavior of the second-order system.

A. Observer design

In this part, the synthesis of an observer consists simply in determining its gain so that the estimation error of the microrobot converges asymptotically to zero.
In order to explain the general procedure of an observer, we will rely on the construction of a Luenberger observer [24], which allows to completely reconstruct the state vector $\chi(t)$. We note by $\hat{\chi}(t)$ the observed variable corresponding to the state vector of the dynamic system that constitutes the observer. The associated Luenberger observer is given by:

$$S_{\hat{x}}: \dot{\hat{\chi}} = A_x \hat{\chi}(t) + B_x u_x + L_x(C_x \chi - C_x \hat{\chi}) \quad (12)$$

The correction term $L_X(Y_X - \hat{Y}_x)$ shows the correction gain also called observation gain where L_X is a constant matrix of appropriate size.

B. Model Predictive Control (MPC)

The strategy known as model based predictive control (MPC) optimize the future and anticipated behavior of the system under consideration based on the inputs[25][26].
The prediction is made from a model of the system over a finite time interval called the h prediction horizon. The control$u_x(t)$ of the output variable $Y_x(t)$ and $X_{ref}(t)$ are consideredconstant $u_x(t) = u_x$ and $X_{ref}(t) = X_{ref}$in the time interval $[t, t+h]$.
where h is the prediction horizon time, by using the Eq. (9), we can formulate the prediction model as follows:

$$x(t+h) = a_{22}u_x(t) + a_{11}v_x(t) + x(t) \qquad (13)$$

where:

$$a_{11} = \left(\frac{e^{a_1 h} - 1}{a_1}\right), a_{22} = \left(\frac{b_1(e^{a_1 h} - 1 - a_1 h)}{a_1^2}\right)$$

The principle of control consists of optimizing performance criterion J_X at each sampling period in order to determine control gains $K = [k_1 k_2]$. Our objective from the point of view trajectory tracking is to minimize not only the error but also the energy of control. This objective is achievable thanks to the following optimization performance criterion:

$$\min(J_x) = e_x^2(t+h) + \gamma \int_0^{t+h} u_x d\tau \qquad (14)$$

where:

$$e_x(t+h) = X_{ref} - x(t+h) \qquad (15)$$

is the prediction error and X_{ref} is the desired value generated by the reference trajectory. By replacing the predicted values of $x(t+h)$ given by (13), therefore the criterion J_x become:

$$J_x = x^2 + x_{ref}^2 - 2xx_{ref} + 2a_{22}xu_x$$

$$+2a_{11}xv_x - 2a_{22}x_{ref}u_x - 2a_{11}v_x x_{ref} \qquad (16)$$

$$+a_{22}^2u_x^2 + 2a_{11}a_{22}u_x v_x + a_{11}v_x^2 + 2h\gamma u_x^2$$

it is minimal at:$\frac{dJ_x}{du_x} = 0$.
where$h$and $\gamma$are non-negative weighting parameter and $u(t) \in \mathcal{R}^2$ are given by:

$$\begin{pmatrix} u_x \\ u_y \end{pmatrix} = \begin{pmatrix} k_1 & 0 \\ 0 & k_1 \end{pmatrix} \begin{pmatrix} e_x \\ e_y \end{pmatrix} + \begin{pmatrix} k_2 \\ k_2 \end{pmatrix} \begin{pmatrix} u_x \\ u_y \end{pmatrix} \qquad (17)$$

where the predictive control law gains are: $k_1 = -\frac{a_{22}}{a_{22}^2 + \gamma h}$ and$k_2 = a_{11}k_1$. These gains will be calculated as follows.

The gain vectors given in (17) of the (MPC) controller are set so that the characteristic polynomial of $\frac{X(p)}{X_{ref}(p)} = \frac{k_1'}{p^2 + k_2' P + k_1'}$has two eigenvaluesplaced in $P_1, P_2 < 0$, we can verify that:

$$\begin{cases} k_1' = w_0^2 \\ k_2' = 2\zeta w_0 \end{cases} \qquad (18)$$

where:$k_1' = \frac{k_1}{m}$, $k_2' = \frac{k_2}{m} - a_1$

The block diagram of the closed-loop (MPC) system can be presented as shown in (Fig.5).

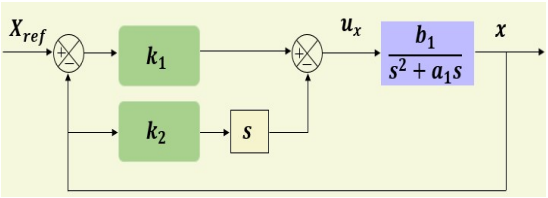

Fig. 5 Equivalent block diagram

4. Simulation and Results

In this Section, the effectiveness of the proposed control strategy, given by Fig. 4, In this section, the effectiveness of the proposed control strategy, given in Figure 5, is evaluated by simulations. The parameters of the microrobot, controller, and observer are shown in Table 1.

Designation	Symbol	Value
Fluid viscosity	η	$16.10^{-3}[pa.s]$
Fluid density	ρ	$8\ [g\ cm^{-2}]$
Robot density	ρ_f	$8\ [g\ cm^{-2}]$
Robot radius	r	$4.908710^{-3}\ [m]$
Blood vessel radius	R	$2.10^{-3}[m]$
Magnetization	M	$1.950.10^{6}\ [A\ m^{-1}]$
Time prediction	h	$0.05\ [s]$
Weight factor	γ	$1.9\ 10^{-6}$
Gain controller	k_1, k_2	8.411610^{-5} 1.378410^{-5}
Gain observer	$L_x = L_y$	$[0.0127 \quad 56.6385]^T$

Table 1Microrobot, controller and observerparameter values.

The initial conditions of the state vector of the microrobot model and the estimated state vector are chosen as follows:

- $\chi(0) = 10^{-3}[-14 \quad 0 \quad 2 \quad 0]$,
- $\hat{\chi}(0) = 10^{-3}[-13 \quad 0 \quad 2.2 \quad 0]$

The simulation results obtained are given by (Fig.6), (Fig.7), (Fig.10) and (Fig.11). It is clear that, the proposed control strategy forces the microrobot to follow the 2D desired trajectory generated by joystick device.

Also, these results clearly show the effectiveness of the Luenberger observer in recovering the microrobot state. We observe that the estimated state variables of the microrobot converge to the real state variables. This is confirmed both by the position and velocity estimation errors(see Fig.9 and Fig.12).

Therefore, we have selected thecorresponding parameters h and γ so that the maximum magnetic force input $(F_{mx}, F_{my})$is around to$10^{-5}N$. Let us take $w_0 = 1.8343\ \mathrm{rad/s}$, replacing this last value in (18), finally the predictive control law gains values are: $(K_1 = 8.4116\ 10^{-6}$and $K_2 = 1.3784\ 10^{-6}$ (see table1), as can be seen on (Fig.6) and (Fig.7), the real trajectory of the microrobot tracks the trajectory generated by the Novint Falcon 2D joystick. This is confirmed both by the position and velocity tracking errors(see Fig.8).

Fig.13 shows the magnetic force control inputs on the $\vec{\imath}$ and $\vec{k}$ axis, which were obtained using the MPC control. It can be seen that using this control approach, the power consumption is lower than $10^{-5}\ N$.

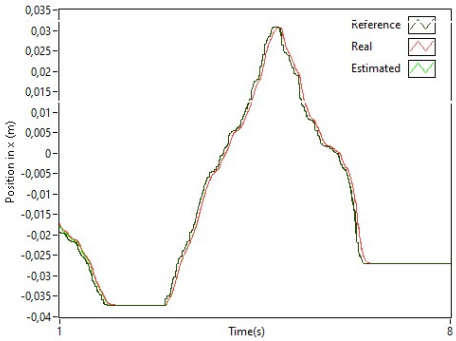

Fig.6Actual, reference and estimated position of the microrobot along the $\vec{\imath}$ and $\vec{k}$ axis.

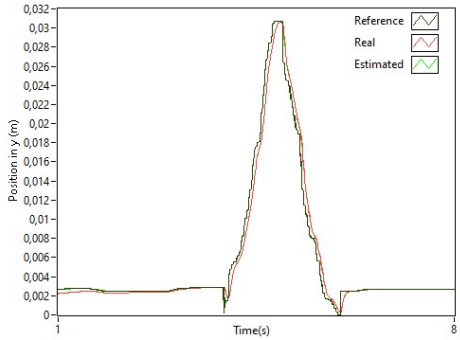

Fig.7Actual, reference and estimated position of the microrobot along the $\vec{\imath}$ and $\vec{k}$ axis.

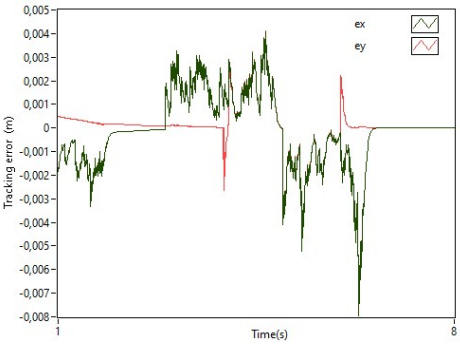

Fig. 8Error between actual and reference position of the microrobot along the $\vec{\imath}$ and $\vec{k}$ axis.

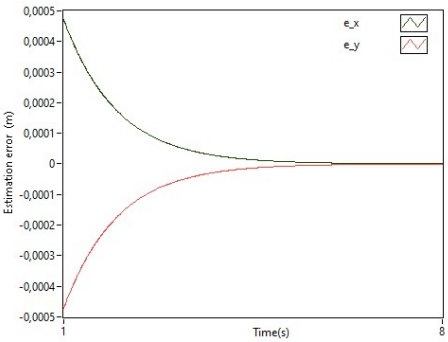

Fig. 9Error between actual and estimated position of the microrobot along the $\vec{\imath}$ and $\vec{k}$ axis.

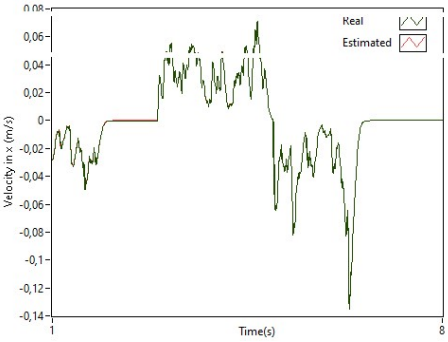

Fig. 10Actual and estimated velocity of the microrobot along the $\vec{\imath}$.

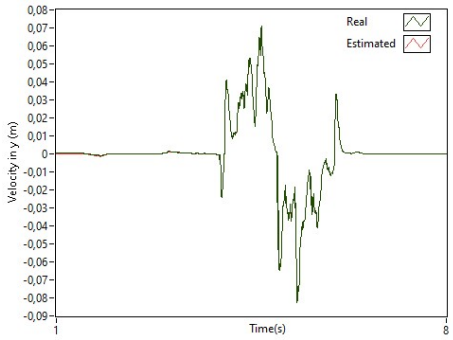

Fig. 11Actual and estimated velocity of the microrobot along the $\vec{k}$ axis

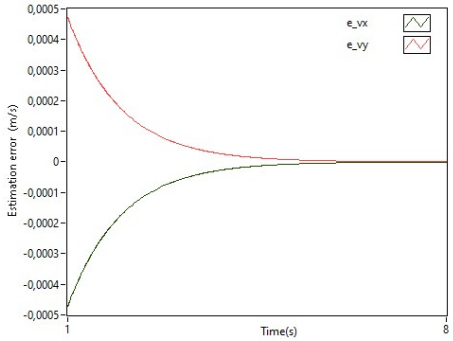

Fig. 12Error between actual and estimated velocity of the microrobot along the $\vec{i}$ and $\vec{k}$ axis.

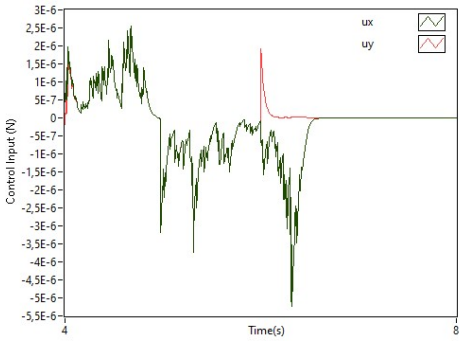

Fig. 13Evolution of the manipulated variables (controls)

5. Discussion

Besides, based on the results obtained (see Figures 6, 7, 10, and 11), the proposed solution i.e., the interaction between the joystick and the model predictive control, is clearly conceivable in complex vascular structures.

6. Conclusion

The present paper proposes a new approach of trajectory tracking for a microrobot navigating in blood vessel. The proposed architecture of control is an observer-based model predictive control (MPC) for a microrobot. The preplanned trajectory is generated via a joystickdevice, and it is estimated using a Luenberger observer. We considered the dynamic model of this microrobot in 2D fluidic environment, and it is linear. Based on this linear model, we developed a model predictive control approach and their parameters (h: the prediction time horizon, γ: the weight factor) are computed, so that the closed loop system has a specific behavior. The obtained simulation results show the efficiency of the proposed approach in termed of trajectory tracking. Future work is aimed to validate the proposed approach of control on areal microrobot for trajectory tracking.

References

[1] K. E. Peyer, L. Zhang, and B. J. Nelson, “Bio-inspired magnetic swimmingmicrorobots for biomedical applications,” Nanoscale, vol. 5,no. 4, pp. 1259–1272, 2013.

[2] J. Dobson, “Magnetic nanoparticules for drug delivery,”Drug developmentresearch, vol. 67, no. 1, pp. 55–60, 2006.

[3] M. Larbi, E.-H. Guechi, A. Chah, A. Maidi, and K. Belharet, “Sliding mode observer of a two-agent microrobotic system,” in 2022 5th International Conference on Advanced Systems and Emergent Technologies (IC ASET). IEEE, 2022, pp. 268–273.

[4] K. Meng, Y. Jia, H. Yang, F. Niu, Y. Wang, and D. Sun,“Motionplanning and robust control for the endovascularnavigation of amicrorobot,” IEEE Transactions on Industrial Informatics, vol. 16,no. 7, pp. 4557–4566, 2019.

[5] W. Ma, M. Xu, Z. Zhong, X. Li, and Z. Huan, “Closed-loop control fortrajectory tracking of a microparticle based on input-to-state stabilitythrough an electromagneticmanipulation system,” IEEE Access, vol. 8,pp. 46 537–46 545, 2020.

[6] K. Belahret, D. Folio, and A. Ferreira, “Endovascular navigation of aferromagnetic microrobot using mri-based predictive control,” in 2010IEEE/RSJ International Conference on Intelligent Robots and Systems.IEEE, 2010, pp. 2804–2809.

[7] K. Belharet, D. Folio, and A. Ferreira, “Control of a magnetic microrobot navigating in microfluidicarterial bifurcations through pulsatile and viscous flow,” in 2012IEEE/RSJ International Conference on Intelligent Robots and Systems.IEEE, 2012, pp. 2559–2564.

[8] K. Belharet, D. Folio, and A. Ferreira, “3d mri-based predictive control of a ferromagnetic microrobotnavigating in blood vessels,” in 2010 3rd IEEE RAS & EMBS InternationalConference on Biomedical Robotics and Biomechatronics.IEEE, 2010, pp. 808–813.

[9] S. Tamaz, R. Gourdeau, A. Chanu, J.-B. Mathieu, and S. Martel,“Real-time mri-based control of a ferromagnetic core for endovascularnavigation,” IEEE Transactions on Biomedical Engineering, vol. 55,no. 7, pp. 1854–1863, 2008.

[10] L. Sadelli, M. Fruchard, and A. Ferreira, “2d observer-based controlof a vascular microrobot,” IEEE Transactions on Automatic Control,vol. 62, no. 5, pp. 2194–2206, 2016.
[11] L. Arcese, M. Fruchard, and A. Ferreira, “Nonlinearmodeling androbust controller-observer for a magneticmicrorobot in a fluidicenvironment using mri gradients,” in 2009 IEEE/RSJ InternationalConference on Intelligent Robots and Systems. IEEE, 2009, pp. 534–539.
[12] T. Xu, J. Yu, X. Yan, H. Choi, and L. Zhang, “Magnetic actuation-based motion control for microrobots: Anoverview,” Micromachines, vol. 6, no. 9, pp. 1346–1364, 2015.
[13] Z. e. B. F. e. N. B. J. Abbott, Jake J et Nagy, “La robotiquedansle petit, partie i: la microbotique,” IEEE Robotics &AutomationMagazine, vol. 14, pp. 92–103.
[14] A. Ferreira, C. Cassier, and S. Hirai, “Automatic microassemblysystem assisted by vision servoing and virtual reality,” IEEE/ASMEtransactions on mechatronics, vol. 9, no. 2, pp. 321–333, 2004.
[15] P. Renon, C. Yang, H. Ma, and R. Cui, “Haptic interactionbetweenhuman and virtual icub robot using novint falcon with chai3d andmatlab,” in Proceedings of the 32nd Chinese Control Conference.IEEE, 2013, pp. 6045–6050.
[16] D. Montero, M. P´aez, and S. Salinas, “Teleoperationprototype using novint falcon haptic interfaces.”
[17] S. Martin and N. Hillier, “Characterisation of the novintfalconhaptic device for application as a robot manipulator,” in AustralasianConference on Robotics and Automation(ACRA). Citeseer, 2009, pp.291–292.
[18] R. B. Ventura, A. Rizzo, O. Nov, and M. Porfiri, “A 3d printingapproach toward targeted intervention intelerehabilitation,” Scientificreports, vol. 10, no. 1, pp. 1–13, 2020.
[19] J. Aleotti, G. Micconi, S. Caselli, G. Benassi, N. Zambelli,M. Bettelli,and A. Zappettini, “Detection of nuclear sourcesby uav teleoperationusing a visuo-haptic augmented realityinterface,” Sensors, vol. 17,no. 10, p. 2234, 2017.
[20] G. Bouyer, A. Chellali, and A. Lecuyer, “Inducing self-motion sensationsin driving simulators using force-feedbackand haptic motion,”in 2017 IEEE Virtual Reality (VR). IEEE,2017, pp. 84–90.
[21] K. B. Yesin, K. Vollmers, and B. J. Nelson, “Modeling and control ofuntethered biomicrorobots in a fluidic environmentusing electromagneticfields,” The International Journal ofRobotics Research, vol. 25,no. 5-6, pp. 527–536, 2006.
[22] K. Belharet, D. Folio, and A. Ferreira, “Mri-based microrobotic systemfor the propulsion and navigation of ferromagnetic microcapsules,”Minimally Invasive Therapy & Allied Technologies, vol. 19, no. 3, pp.157–169, 2010.
[23] L. E. Trucios, M. Tavakoli, and K. Adams, “Adaptivetracking controlfor task-based robot trajectory planning,” in 2020 IEEE InternationalConference on Systems, Man, andCybernetics (SMC). IEEE, 2020,pp. 4256–4260.
[24] D. Luenberger, “An introduction to observers,” IEEETransactions onautomatic control, vol. 16, no. 6, pp. 596–602, 1971.
[25] E.-H. Guechi, S. Bouzoualegh, L. Messikh, and S. Bla˘zic, “Modelpredictive control of a two-link robot arm,” in 2018International Conferenceon Advanced Systems and Electric Technologies (IC ASET).IEEE, 2018, pp. 409–414.
[26] E.-H. Guechi, S. Bouzoualegh, Y. Zennir, and S. Blazic,“Mpc controland lq optimal control of a two-link robot arm: A comparative study,”Machines, vol. 6, no. 3, p. 37, 2018.